THE GEOLOGICAL SOCIETY OF AMERICA®

Water concentration profiles in natural mantle orthopyroxenes: A geochronometer for long annealing of xenoliths within magma

Zhen-Zhen Tian[1], Jia Liu[1]*, Qun-Ke Xia[2], Jannick Ingrin[3], Yan-Tao Hao[2], and Depecker Christophe[3]
[1]Chinese Academy of Sciences Key Laboratory of Crust-Mantle Materials and Environments, School of Earth and Space Science, University of Science and Technology of China, Hefei 230026, China
[2]School of Earth Sciences, Zhejiang University, Hangzhou 310027, China
[3]Unité Matériaux et Transformations (UMET), UMR CNRS 8207, Université de Lille 1, Bâtiment C6, Villeneuve d'Ascq 59655, France

ABSTRACT

Both mantle-derived clinopyroxene and orthopyroxene are generally homogeneous in water concentration, while water content in the coexisting olivine is affected by partial or complete loss during the ascent of the hosting magma. Here, we report the first record of water content profiles (higher water in the cores than in the rims) in natural orthopyroxene grains in peridotite xenoliths hosted by Cenozoic alkali basalts in Tianchang volcano, eastern China. The water contents of the coexisting clinopyroxene grains are homogeneous and are twice that measured in the cores of orthopyroxene grains, confirming previous chemical equilibrium between the two pyroxenes. The olivines (ol) are nearly dry (~0 ppm). These observations demonstrate that H diffusion in mantle orthopyroxene (opx) is faster than in clinopyroxene (cpx), and the relative mobility of H in each mineral phase could be quantified as: $\tilde{D}_{ol} > 10\tilde{D}_{opx} > 1000\tilde{D}_{cpx}$ (where $\tilde{D}$ is the chemical diffusion coefficient of hydrogen). Combining this with experimental diffusion coefficients from the literature, we infer that (1) the xenoliths remained in contact with the magma below 900 °C for several months, and (2) clinopyroxene remains the more reliable recorder of water from depth, and orthopyroxene should be used more cautiously but can be considered with olivine for tracing slow transport and cooling of magma.

INTRODUCTION

Trace amounts of water structurally bound as point defects in normally anhydrous minerals (NAMs) have a significant effect on the chemical and physical properties of Earth's mantle minerals and rocks (e.g., Mackwell et al., 1985; Asimow et al., 2004; Gaetani and Grove, 1998; Yoshino et al., 2012). Many studies have investigated the water concentration in minerals from mantle-derived peridotite xenoliths hosted by kimberlites and alkali basalts (continental and oceanic), as well as tectonically exhumed oceanic peridotites (e.g., Bell and Rossman, 1992; Ingrin and Skogby, 2000; Demouchy et al., 2006, 2015; Xia et al., 2010; Peslier et al., 2010; Warren and Hauri, 2014; Hesse et al., 2015; Denis et al., 2015; Peslier and Bizimis, 2015). In some cases, olivines (xenocrysts or hosted in xenolithic peridotites) display no detectable structural OH or obvious water concentration profiles, which has usually been explained as the result of complete or partial water loss through diffusion during magma ascent (Demouchy et al., 2006; Xia et al., 2010; Peslier and Luhr, 2006; Doucet et al., 2014). In contrast, the water within mantle-derived clinopyroxene (cpx) and orthopyroxene (opx) single crystals is usually homogeneous and shows no diffusion profile. The apparent water concentration ratio between cpx and opx is commonly close to 2 ($R_{cpx/opx}$ = 2.1, N = 327; Demouchy and Bolfan-Casanova, 2015; Xia et al., 2010; Denis et al., 2015), a value that was proposed to reflect equilibrium partitioning.

On one hand, although some cpx phenocrysts in basalts may have lost part of their water (Weis et al., 2015), the homogeneous distribution of water within mantle-derived pyroxenes, and the similar water partitioning between cpx and opx comparable with experimental values indicate that both cpx and opx reliably record equilibrium water concentration (Bell and Rossman, 1992; Grant et al., 2007; Xia et al., 2010; Warren and Hauri, 2014; Denis et al., 2015; Hesse et al., 2015; Peslier and Bizimis, 2015). On the other hand, water profiles in mantle-derived olivine have been used to estimate the ascent rate of the hosting magma from the mantle (e.g., Demouchy et al., 2006; Peslier and Luhr, 2006; Denis et al., 2015). However, most previous studies reporting water profiles in olivine assumed a simple case, where the H diffusion occurs during transport from mantle depths, and the shallow cooling history near or after eruption has a negligible effect on the observed profiles.

In this study, we present the first unpolarized Fourier transform infrared spectroscopy (FTIR) observations of water concentration profiles in natural opx grains from peridotite xenoliths hosted by continental alkali basalts. Combined with the water distribution in the coexisting cpx and ol, these water concentration profiles were used to constrain the H diffusion mechanism in minerals and the annealing history of the mantle-derived xenoliths in the hosting magma.

SAMPLES AND METHODS

The studied samples are 15 spinel-lherzolite xenoliths and one harzburgite xenolith hosted by Cenozoic basanites from Tianchang volcano in eastern China (see Fig. DR1 in the GSA Data Repository[1]). The samples were collected from an open-pit quarry, ~10 m below the surface of the lava flow (Fig. DR1B). A few cpx and opx grains showed evidence of a little alteration in their rims, but otherwise no modal hydrous minerals or deformation-induced fabrics were observed (Fig. DR2). In addition, the samples showed no evidence of melt infiltration by the host magma. The Mg# [= 100 × Mg/(Mg + Fe)] values of olivines in these xenoliths ranged from 89.0 to 91.4 (Hao et al., 2016; Table DR1) and fell within the range of published data for peridotite xenoliths hosted by Cenozoic basalts from eastern China (e.g., Xia et al., 2010; Fig. DR3). The cpx exhibited $(La/Yb)_n$ (where n represents primitive mantle normalization) values varying from 0.05 to 11.57 (Table DR4). The equilibrium temperatures were estimated to be ~800–1050 °C (at ~15 kbar; Hao et al., 2016; Table DR4). Water contents of ol, cpx, and opx were quantitatively determined by FTIR spectroscopy (Hao et al., 2016; see the Data Repository), using the approach proposed by Kovács et al. (2008). A Spotlight 200 PerkinElmer FTIR (unpolarized beam) was used in transmission mode to conduct line analyses on double polished sections to check the

*E-mail: liujia08@ustc.edu.cn

[1]GSA Data Repository item 2017022, methods and additional data, is available online at www.geosociety.org/pubs/ft2017.htm, or on request from editing@geosociety.org.

homogeneity of water concentration in opx and cpx grains. Backscatter-electron images (BSEs) and linear composition profiles (Mg, Fe, Ca) were obtained to check the major-element homogeneity in olivine and opx. Details of FTIR profile analyses and linear composition analyses can be found in the GSA Data Repository.

RESULTS

In all samples, the olivines have no detectable OH infrared bands (Fig.1A). The OH bands of the pyroxenes are comparable to those observed in peridotite pyroxenes throughout the world (Demouchy and Bolfan-Casanova, 2015, and references therein; Fig. 1A). Profile analyses show that the opx grains in each xenolith have systematically higher water concentration in the cores than in the rims (Figs. 1 and 2; Fig. DR4; Table DR5). The occurrence of water gradients is independent of the Mg# of opx, the $(La/Yb)_n$ of cpx, which may vary from sample to sample (Tables DR4 and DR5), and the location within the xenolith (in the center or edge). This indicates that H gradients in opx are prevalent in all samples and not linked to mantle metasomatism affecting these parameters. Furthermore, the opx grains are otherwise homogeneous in major elements, and no Mg# gradients associated with the H gradients are observed (Fig. 2A). In contrast, FTIR measurements show that the cpx grains exhibit rather

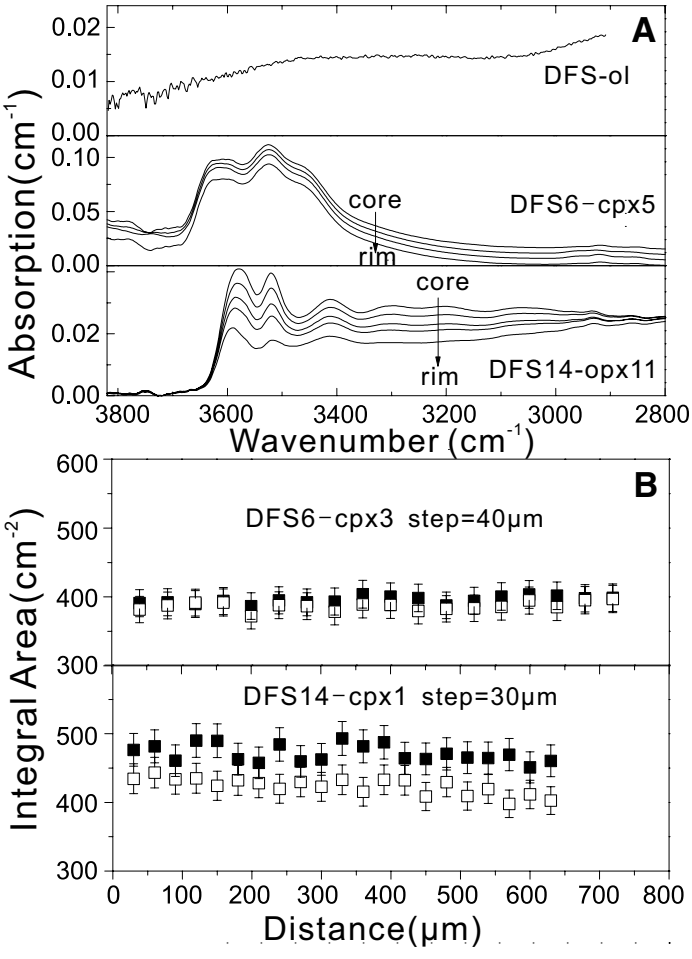

Figure 1. A: Typical infrared absorbance spectra of OH bands in olivine (ol), clinopyroxene (cpx), and orthopyroxene (opx) in Tianchang (China) peridotite. Spectra have been normalized to a thickness of 1 cm and vertically shifted for comparison. B: Water concentration profiles in cpx grains. Integral absorptions are normalized to a thickness of 1 cm. Two baseline correction strategies were conducted for comparison (relative uncertainty is 5%). Electron probe micro-analysis (EPMA) along the same profiles show that cpx grains have homogeneous major-element compositions (Table DR2 [see footnote 1]).

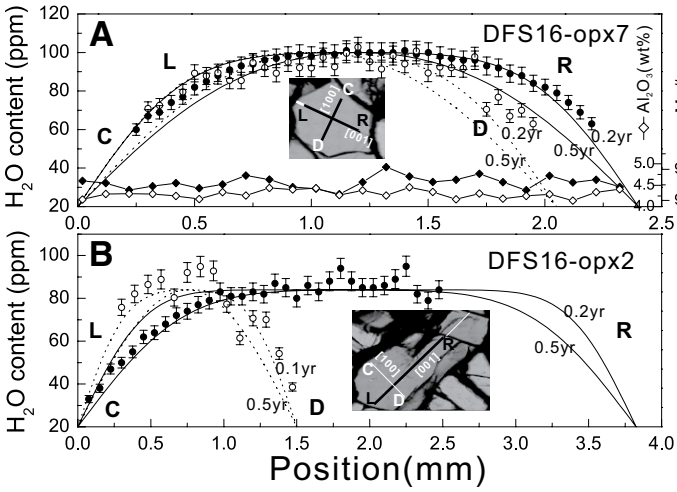

Figure 2. Water concentration profiles and diffusion modeling for two orthopyroxenes (opx) from Tianchang (China) peridotite. See the Data Repository (see footnote 1) for method used to calculate water contents. Error bars on water content represent a relative uncertainty of 5%. Solid and dashed lines show fitting results (3-D model), and numbers nearby are fitted time (yr). In calculations, diffusion along different direction is assumed to be 10^{-14} m²/s (isotropic). Additional details of fitting can be found in the Data Repository. White lines in inset pictures mark spots not processed for calculation of water content due to contamination. For DFS16-opx7, Mg# and Al_2O_3 profiles are shown for comparison (see Table DR3 for full electron probe micro-analyzer data). Additional opx profiles are shown in Figure DR4 and Table DR6 in the Data Repository. L-R and C-D mark the direction of the profiles shown in the inset images.

homogeneous water distribution at least ~60 μm away from the grain boundary (Fig. 1B), even if these grains are considerably smaller than opx grain sizes (the typical diameter of cpx and opx was 500–1500 μm and >2500 μm, respectively). The average water concentrations of cpx and opx in peridotites are 72–283 ppm H_2O and 36–137 ppm H_2O, respectively (Hao et al., 2016; Table DR5). In addition, the apparent partition coefficients of water in cpx and the core of opx for Tianchang xenoliths are close to 2 ($R_{cpx/opx}$ = 2.02; Fig. DR5; Hao et al., 2016), which is very close to the average partition coefficient measured in mantle xenoliths showing no diffusion profile (e.g., Grant et al., 2007; Denis et al., 2015; Peslier and Bizimis, 2015). From this, we suggest that the H_2O contents in the cpx and the core of opx from the Tianchang peridotite xenoliths are in equilibrium, while the rim of opx had lost part of its water through diffusion.

BSE imaging coupled with profile analyses by electron probe micro-analyzer (EPMA) shows that the olivines in contact with the host magma exhibit Fe-Mg and Ca diffusion rims (Fig. DR6). Based on the experimental diffusion rates for Fe-Mg interdiffusion and Ca cationic diffusion in olivine (Dohmen and Chakraborty, 2007; Coogan et al., 2005), the estimated diffusion time periods at 1200 °C (the typical liquidus temperature for alkali basalts) and 900 °C (during the cooling of alkali basalts) are ~1.5 yr and 180 yr, respectively (see modeling details in the caption of Fig. DR6).

HYDROGEN DIFFUSIVITY IN PYROXENES AND OLIVINE

All the minerals in the same xenolith experience the same pressure–temperature–time–water fugacity (P-T-t-f_{H_2O}) path during their transport to the surface. According to the observed water concentration profiles in opx (Fig. 2), the characteristic diffusion length (d) is equal to ~0.75–1.0 mm (corresponding roughly to 90% of the complete profile; Zhang, 2008). In cpx, an upper limit of 0.06 mm can be deduced from the absence of a diffusion profile in the FTIR measurements at this scale (Fig. 1B). Since all the olivines are dry, the characteristic diffusion length is necessarily larger

than the grain size (3 mm in diameter). Thus, $d_{ol} > 3.5d_{opx} > 50d_{cpx}$, and the respective H diffusivity follows the relationship $\tilde{D}_{ol} > 10\tilde{D}_{opx} > 1000\tilde{D}_{cpx}$ (where $\tilde{D}$ is the chemical diffusion rate of hydrogen in minerals). This estimate is similar to the results from three-dimensional modeling (Fig. DR7).

Data from the literature show that three types of diffusion mechanisms are involved in H diffusion (for references, see the caption of Fig.3): (1) H self-diffusion deduced from H-D exchange experiments, which is considerably faster in cpx than in opx ($D_{H\text{-}D}$, upper green and yellow area in Fig. 3); (2) H chemical diffusion controlled by the mobility of polarons (involving the oxidation-reduction of iron), the rates of which are comparable for the three minerals olivine, opx, and cpx ($D_{H\text{-}pp}$ coefficients in Fig. 3); and (3) H chemical diffusion controlled by the mobility of metal vacancies, which involve the formation and destruction of octahedral vacancies. The last mechanism is the only one for which diffusion in olivine and opx is significantly faster than in cpx ($D_{H\text{-}pv}$ and low green and yellow area in Fig. 3). Thus, it is the only one that can satisfactorily explain the observed profiles in opx, as was previously suggested from diffusion profiles observed in olivine (e.g., Demouchy et al., 2006; Grant et al., 2007; Peslier and Bizimis, 2015).

The details of the mechanisms of H diffusion involving metal vacancies in natural pyroxenes are still not fully elucidated and need more investigation, as shown by the complexity of the compiled diffusion data presented in Figure 3. The key data for the interpretation of the relative H diffusivity in opx and cpx ($\tilde{D}_{opx} > 100\tilde{D}_{cpx}$) are highlighted by the thick lines: a thick green line for the diffusion in Fe-poor diopside and thick yellow lines for the diffusion in opx. These data are directly comparable, since they were obtained in the same conditions (Sundvall et al., 2009a, 2009b; Stalder and Skogby, 2003). Figure 3 also suggests that, where this diffusion mechanism dominates, lower temperatures (lower than 900 °C) are essential to allow H diffusion in opx to be nearly one order of magnitude slower than

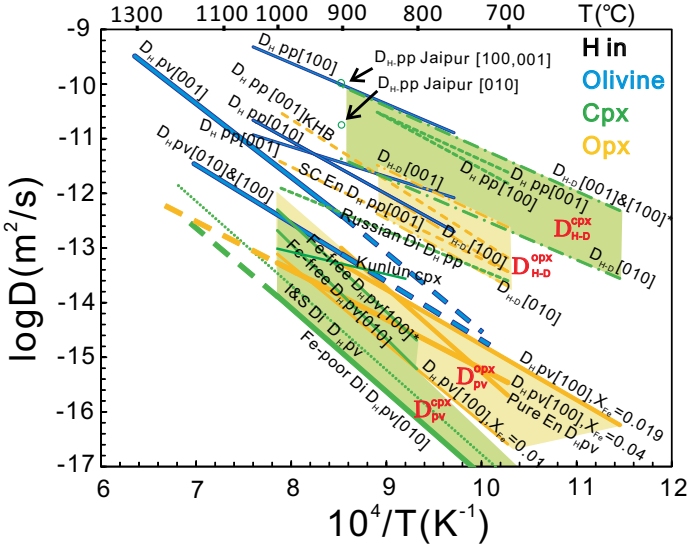

Figure 3. Arrhenius diagram of hydrogen diffusion in olivine (ol), clinopyroxene (cpx), and orthopyroxene (opx). $D_{H\text{-}D}$ represents hydrogen self-diffusivity, $D_{H\text{-}pv}$ and $D_{H\text{-}pp}$ represent effective hydrogen diffusivity controlled by mobility of metal vacancies and electronic holes, respectively. Dotted green line (I&S Di $D_{H\text{-}pv}$) is effective H diffusivity extrapolated from mobility of metal vacancies from Guilhaumou et al. (1998). Dashed ends of solid broad lines were created by extrapolating experimental data to lower or higher temperatures. Recent experimental H diffusivity data in Kunlun and Jaipur diopsidic cpx from Ferriss et al. (2016) are also shown. Other data are from Ingrin and Blanchard (2006), Demouchy and Bolfan-Casanova (2015, and references therein), Woods et al. (2000), Stalder and Behrens (2006), Stalder and Skogby (2007), Stalder et al. (2007), and Sundvall et al. (2009 a, 2009b). KHB—Kilbourne Hole; SC En—San Carlos enstatite; En—enstatite; Di—diopside; Russian Di—Russian gem-quality diopside (Ingrin et al. 1995).

that in olivine but about two orders of magnitudes faster than that in cpx. Therefore, considering the present knowledge on H diffusion in pyroxenes, we infer that the water contents observed in opx were obtained because the xenoliths remained in contact with a partially degassed magma around 900 °C (or below) for a long period of time. If we assume the temperature to be around 900 °C, the expected H diffusion rate in opx is around 10^{-14} m²/s. This leads to an estimated annealing time of ~0.2–0.5 yr (see Fig. 2).

The fact that the xenoliths remained in contact with the magma for a long time before it cooled is also suggested by the Fe-Mg-Ca diffusion profiles observed in olivine in contact with the magma. As shown in Figure DR6, the formation of Fe-Mg and Ca concentration profiles in olivine would require the peridotite xenolith to be stored in a magma at 1200 °C for at least 1.5 yr. However, at this stage, if the magma were degassed, the cpx would have lost more than 90% of its initial water content, even if the slowest diffusion rate for cpx is assumed. The difference by several orders of magnitude between the diffusion coefficients of cations in olivine and the diffusion coefficients of hydrogen in pyroxenes suggests that the diffusion of H and cations in Tianchang xenoliths were two asynchronous events. One likely scenario to explain the observed H diffusion in opx and Fe-Mg-Ca diffusion in olivine is: (1) The xenoliths were trapped in an undegassed magma chamber in the deep or shallow crust for a time period close to 1 yr, which allowed cation diffusion in olivine; and (2) H diffusion occurred later, when xenoliths reached the near surface in a degassed slowly cooling lava flow. This scenario is highly probable, given that it is well known that mantle-derived xenoliths in intraplate alkali lavas are finally taken to the surface after a long residence (hundred days to several years) in deep magma chambers. This behavior has been demonstrated, for example, in basanite from the Massif Central and West Eifel (Shaw, 2004; Oeser et al., 2015).

IMPLICATIONS

This study confirms that H diffusion in both cpx and opx from the Tianchang peridotites is controlled by the mobility of metal vacancies (broad colored lines in Fig. 3). At temperatures from 1000 °C to 1200 °C, H diffusivity controlled by metal vacancies in both cpx and opx is one or two orders of magnitude lower than that in olivine (Fig. 3). This observation corresponds to characteristic diffusion lengths that are between 3 and 10 times smaller in these phases than in olivine. In these conditions, it is surprising that no diffusion profiles have been reported in pyroxenes from xenoliths with dry olivines (characteristic diffusion length larger than 3 mm; Xia et al., 2010; Peslier and Luhr, 2006). This may indicate that the previously reported H diffusion profiles in olivine, with no equivalent diffusion profiles observed in the coexisting pyroxenes, were not necessarily formed during the ascent of the hosting magma from depth. Instead, they could have been developed at lower temperature during the last stage of transport from a shallow magma chamber to the surface or during cooling after eruption. Ferriss et al. (2016) also reached a similar conclusion, i.e., that water zonation profiles observed in olivine are mostly related to water exsolving during the final stage of ascent of the magma. Their conclusion was based on the results of dehydration experiments performed on cpx single crystals with different Fe contents, showing that H diffusion in cpx is too fast to avoid partial loss if degassing occurs all along transport from mantle depths. However, we have reached a different conclusion based on diffusion in cpx from xenoliths: (1) H diffuses out of mantle cpx at a much slower rate than they proposed (at least 3 orders of magnitude below olivine, compared to 1–2 orders of magnitude), and (2) diffusion by oxidation-reduction of iron is not efficient enough in this context; instead diffusion is most likely controlled by metal- vacancy diffusivity.

These observations show that time spent in the degassed magma during the late stages of transport or after eruption has a drastic effect on water preservation in mantle xenoliths. Therefore, (1) the reason why other xenoliths do not exhibit H zonation in pyroxenes would be that they have been cooled more efficiently during and after eruption (for instance, lack

of shallower magma chambers, and the hosting lava flow is thin). (2) An oversimplified model that assumes a progressive, constant degassing from depth would lead to an overestimation of the rate of magma ascent. Considering both that olivine usually experiences partial or complete water loss (Demouchy et al., 2006; Peslier and Luhr, 2006; this study) and that the H diffusion coefficient of cpx could be approximately two orders of magnitude slower than that of opx, we also suggest that cpx is the most robust recorder of water content and hydrogen isotopic signatures from depth.

ACKNOWLEDGMENTS

We thank Hai-Wei Ni and Li Zhang for their help during the water profile analysis with the PE imaging system. We are also grateful to Wen-Long Liu for his help with the EBSD analysis. Comments from S. Demouchy, Martin J. Streck, Henrik Skogby, Luc S. Doucet, editor J. Brendan Murphy, and an anonymous reviewer were very beneficial to this paper. Kevin Grant is thanked for his comments and corrections to the article. Liu thanks Wei Sun, Qian Hu, and Xiaoyu Sun for their helpful discussion about diffusion modeling. This work was supported by the National Science Foundation of China, grants 41225005 and 41502041.

REFERENCES CITED

Asimow, P.D., Dixon, J.E., and Langmuir, C.H., 2004, A hydrous melting and fractionation model for mid-ocean ridge basalts: Application to the Mid-Atlantic Ridge near the Azores: Geochemistry Geophysics Geosystems, v. 5, p. Q01E16, doi:10.1029/2003GC000568.

Bell, D.R., and Rossman, G.R., 1992, Water in Earth's mantle—The role of nominally anhydrous minerals: Science, v. 255, p. 1391–1397, doi:10.1126/science.255.5050.1391.

Coogan, L.A., Hain, A., Stahl, S., and Chakraborty, S., 2005, Experimental determination of the diffusion coefficient for calcium in olivine between 900°C and 1500°C: Geochimica et Cosmochimica Acta, v. 69, p. 3683–3694, doi:10.1016/j.gca.2005.03.002.

Demouchy, S., and Bolfan-Casanova, N., 2015, Distribution and transport of hydrogen in the lithospheric mantle: A review: Lithos, v. 240–243, p. 402–425, doi:10.1016/j.lithos.2015.11.012.

Demouchy, S., Jacobsen, S.D., Gaillard, F., and Stern, C.R., 2006, Rapid magma ascent recorded by water diffusion profiles in mantle olivine: Geology, v. 34, p. 429–432, doi:10.1130/G22386.1.

Demouchy, S., Ishikawa, A., Tommasi, A., Alard, O., and Keshav, S., 2015, Characterization of hydration in the mantle lithosphere: Peridotite xenoliths from the Ontong-Java Plateau as an example: Lithos, v. 212, p. 189–201, doi:10.1016/j.lithos.2014.11.005.

Denis, C.M.M., Alard, O., and Demouchy, S., 2015, Water content and hydrogen behaviour during metasomatism in the uppermost mantle beneath Ray Pic volcano (Massif Central, France): Lithos, v. 236–237, p. 256–274, doi:10.1016/j.lithos.2015.08.013.

Dohmen, R., and Chakraborty, S., 2007, Fe-Mg diffusion in olivine II: Point defect chemistry, change of diffusion mechanisms and a model for calculation of diffusion coefficients in natural olivine: Physics and Chemistry of Minerals, v. 34, p. 409–430, doi:10.1007/s00269-007-0158-6.

Doucet, L.S., Peslier, A.H., Ionov, A.I., Brandon, A.D., Golovin, A.V., Goncharov, A.G., and Ashchepkov, I.V., 2014, High water contents in the Siberian cratonic mantle linked to metasomatism: An FTIR study of Udachnaya peridotite xenoliths: Geochimica et Cosmochimica Acta, v. 137, p. 159–187, doi:10.1016/j.gca.2014.04.011.

Ferriss, E., Plank, T., and Walker, D., 2016, Site-specific hydrogen diffusion rates during clinopyroxene dehydration: Contributions to Mineralogy and Petrology, v. 171, p. 1–24, doi:10.1007/s00410-016-1262-8.

Gaetani, G.A., and Grove, T.L., 1998, The influence of water on melting of mantle peridotite: Contributions to Mineralogy and Petrology, v. 131, p. 323–346, doi:10.1007/s004100050396.

Grant, K., Ingrin, J., Lorand, J.P., and Dumas, P., 2007, Water partitioning between mantle minerals from peridotite xenoliths: Contributions to Mineralogy and Petrology, v. 154, p. 15–34, doi:10.1007/s00410-006-0177-1.

Guilhaumou, N., Dumas, P., Carr, G.L., and Williams, G.P., 1998, Synchrotron infrared microspectrometry applied to petrography in the micron scale range: Fluid chemical analysis and mapping: Applied Spectroscopy, v. 52, p. 1029–1034, doi:10.1366/0003702981944797.

Hao, Y.T., Xia, Q.K., Tian, Z.Z., and Liu, J., 2016, Partial melting control of water contents in metasomatized lithospheric mantle: Evidence from the Tianchang peridotite xenoliths of eastern China: Lithos, v. 260, p. 315–327, doi:10.1016/j.lithos.2016.06.003.

Hesse, K.T., Gose, J., Stalder, R., and Schmadicke, E., 2015, Water in orthopyroxene from abyssal spinel peridotites of the East Pacific Rise (ODP Leg 147: Hess Deep): Lithos, v. 232, p. 23–34, doi:10.1016/j.lithos.2015.06.011.

Ingrin, J., and Blanchard, M., 2006, Diffusion of hydrogen in minerals: Reviews in Mineralogy and Geochemistry, v. 62, p. 291–320, doi:10.2138/rmg.2006.62.13.

Ingrin, J., and Skogby, H., 2000, Hydrogen in nominally anhydrous upper-mantle minerals: Concentration levels and implications: European Journal of Mineralogy, v. 12, p. 543–570, doi:10.1127/ejm/12/3/0543.

Ingrin, J., Hercule, S., Charton, T., 1995, Diffusion of hydrogen in diopside: Results of dehydration experiments: Journal of Geophysical Research: Solid Earth, v.100, p. 15,489–15,499, doi:10.1029/95JB00754.

Kovács, I., Hermann, J., O'Neill, H.S.C., Gerald, J.F., Sambridge, M., and Horvath, G., 2008, Quantitative absorbance spectroscopy with unpolarized light: Part II. Experimental evaluation and development of a protocol for quantitative analysis of mineral IR spectra: The American Mineralogist, v. 93, p. 765–778, doi:10.2138/am.2008.2656.

Mackwell, S.J., Kohlstedt, D.L., and Paterson, M.S., 1985, The role of water in the deformation of olivine single crystals: Journal of Geophysical Research, v. 90, p. 11,319–11,333, doi:10.1029/JB090iB13p11319.

Oeser, M., Dohmen, R., Horn, I., Schuth, S., and Weyer, S., 2015, Processes and time scales of magmatic evolution as revealed by Fe-Mg chemical and isotopic zoning in natural olivines: Geochimica et Cosmochimica Acta, v. 154, p. 130–150, doi:10.1016/j.gca.2015.01.025.

Peslier, A.H., and Bizimis, M., 2015, Water in Hawaiian peridotite minerals: A case for a dry metasomatized oceanic mantle lithosphere: Geochemistry Geophysics Geosystems, v. 16, p. 1211–1232, doi:10.1002/2015GC005780.

Peslier, A.H., and Luhr, J.F., 2006, Hydrogen loss from olivines in mantle xenoliths from Simcoe (USA) and Mexico: Mafic alkalic magma ascent rates and water budget of the sub-continental lithosphere: Earth and Planetary Science Letters, v. 242, p. 302–319, doi:10.1016/j.epsl.2005.12.019.

Peslier, A.H., Woodland, A.B., Bell, D.R., and Lazarov, M., 2010, Olivine water contents in the continental lithosphere and the longevity of cratons: Nature, v. 467, p. 78–81, doi:10.1038/nature09317.

Shaw, C.S.J., 2004, The temporal evolution of three magmatic systems in the West Eifel volcanic field, Germany: Journal of Volcanology and Geothermal Research, v. 131, p. 213–240, doi:10.1016/S0377-0273(03)00363-9.

Stalder, R., and Behrens, H., 2006, D/H exchange in pure and Cr-doped enstatite: Implications for hydrogen diffusivity: Physics and Chemistry of Minerals, v. 33, p. 601–611, doi:10.1007/s00269-006-0112-z.

Stalder, R., and Skogby, H., 2003, Hydrogen diffusion in natural and synthetic orthopyroxene: Physics and Chemistry of Minerals, v. 30, p. 12–19, doi:10.1007/s00269-002-0285-z.

Stalder, R., and Skogby, H., 2007, Dehydration mechanisms in synthetic Fe-bearing enstatite: European Journal of Mineralogy, v. 19, p. 201–216, doi:10.1127/0935-1221/2007/0019-1710.

Stalder, R., Purwin, H., and Skogby, H., 2007, Influence of Fe on hydrogen diffusivity in orthopyroxene: European Journal of Mineralogy, v. 19, p. 899–904, doi:10.1127/0935-1221/2007/0019-1780.

Sundvall, R., Skogby, H., and Stalder, R., 2009a, Dehydration-hydration mechanisms in synthetic Fe-poor diopside: European Journal of Mineralogy, v. 21, p. 17–26, doi:10.1127/0935-1221/2009/0021-1880.

Sundvall, R., Skogby, H., and Stalder, R., 2009b, Hydrogen diffusion in synthetic Fe-free diopside: European Journal of Mineralogy, v. 21, p. 963–970, doi:10.1127/0935-1221/2009/0021-1971.

Warren, J.M., and Hauri, E.H., 2014, Pyroxenes as tracers of mantle water variations: Journal of Geophysical Research–Solid Earth, v. 119, p. 1851–1881, doi:10.1002/2013JB010328.

Weis, F.A., Skogby, H., Troll, V.R., Deegan, F.M., and Dahren, B., 2015, Magmatic water contents determined through clinopyroxene: Examples from the western Canary Islands, Spain: Geochemistry Geophysics Geosystems, v. 16, p. 2127–2146, doi:10.1002/2015GC005800.

Woods, S.C., Mackwell, S., and Dyar, A., 2000, Hydrogen in diopside: Diffusion profiles: The American Mineralogist, v. 85, p. 480–487, doi:10.2138/am-2000-0409.

Xia, Q.K., Hao, Y.T., Li, P., Deloule, E., Coltorti, M., Dallai, L., Yang, X.Z., and Feng, M., 2010, Low water content of the Cenozoic lithospheric mantle beneath the eastern part of the North China craton: Journal of Geophysical Research–Solid Earth, v. 115, p. B07207, doi:10.1029/2009JB006694.

Yoshino, T., Shimojuku, A., Shan, S., Guo, X., Yamazaki, D., Ito, E., Higo, Y., and Funokoshi, K.-I., 2012, Effect of temperature, pressure and iron content on the electrical conductivity of olivine and its high-pressure polymorphs: Journal of Geophysical Research, v. 117, B08205, doi:10.1029–2011JB008774.

Zhang, Y., 2008, Geochemical Kinetics: Princeton, New Jersey, Princeton University Press, 664 p.

Manuscript received 20 September 2016
Revised manuscript received 27 October 2016
Manuscript accepted 27 October 2016

Printed in USA